Journal of Soils and Sediments (2021) 21:3034–3043
https://doi.org/10.1007/s11368-021-03011-z

SOILS, SEC 1 • SOIL ORGANIC MATTER DYNAMICS AND NUTRIENT CYCLING • RESEARCH ARTICLE

Evaluating the effect of soil internal forces on the stability of natural soil aggregates during vegetation restoration

Rentian Ma[1] · **Feinan Hu**[1,2] · **Jingfang Liu**[1] · **Shiwei Zhao**[1,2]

Received: 6 January 2021 / Accepted: 24 June 2021 / Published online: 3 July 2021

Abstract

Purpose Soil aggregate stability associates closely with many environmental and agricultural problems. Some studies using the model aggregates find that soil internal forces exert an important impact on soil aggregate stability. However, the effect of soil internal forces on the stability of natural soil aggregates during vegetation restoration has been little studied.

Methods Five different succession stages (including farmland, grassland, shrubland, early forest, and climax forest) were chosen in the Ziwuling forest region (in the central part of the Loess Plateau, China), and the size distribution and stability of natural soil aggregates under different succession stages were investigated through dry sieving and wet sieving with ethanol and deionized water prewetting.

Results The size distribution of aggregates determined by dry sieving showed decreased first and then increased with decreasing particle size, dominant sizes were 5–1- and < 0.15-mm fractions. The ethanol prewetting treatment showed a distribution similar to that determined by dry sieving. The size distribution of aggregates in deionized water prewetting treatment was mainly < 0.15-mm fractions. Moreover, the mean weight diameter values of farmland, grassland, shrubland, early forest, and climax forest soils determined in ethanol treatment (MWDe) were 4.62, 1.45, 1.31, 1.32, and 1.17 times than those in deionized water treatment (MWDw). In addition, in the fast wetting process, the preservation rate of soil aggregates was higher in 0.5–0.053-mm fractions than in > 0.5-mm fractions. The relative internal force index (RII) of grassland, shrubland, early forest, and climax forest soils decreased by 47%, 54%, 55%, and 64% compared with that of farmland soil, respectively.

Conclusions These findings demonstrate that soil internal forces could significantly break down the aggregates and lead to decreasing water stability of aggregates. The vegetation restoration process decreased the repulsive soil internal forces, thereby decreasing the degree of disintegration of aggregates and consequently increased the water stability of aggregates.

Keywords Aggregate stability · Aggregate size distribution · Ethanol · Soil organic matter · The Loess Plateau

1 Introduction

Vegetation restoration is an effective measure for the ecological environment construction. Its implementation has changed the irrational land use, and facilitated the functional use of the soil–plant system in order to recover soil fertility and improve soil structure (Li and Shao 2006; El Kateb et al. 2013; Bienes et al. 2016). Soil aggregates are the basic units of soil structures, and their stability are highly associated with environmental and agricultural problems, such as degradation of organic matter, water storage and movement, carbon turnover, biological activity, crop growth, and soil erosion (Tisdall and Oades 1982; Lenka et al. 2012; Liu et al. 2014; Zhu et al. 2017). Hence, exploring soil aggregate stability is essential for maintaining soil function in agricultural production and terrestrial material cycling.

Previous studies on the mechanisms of soil aggregate stability mainly focused on the slaking effect, differential swelling, raindrop impact, and physicochemical dispersion (Le Bissonnais 1996; Kinnell 2005). Recently, soil internal

Responsible editor: Zhihong Xu

✉ Feinan Hu
hufeinan-629@163.com; hufn@nwafu.edu.cn

[1] State Key Laboratory of Soil Erosion and Dryland Farming On the Loess Plateau, Northwest A&F University, Yangling 712100, China

[2] Institute of Soil and Water Conservation, Chinese Academy of Sciences and Ministry of Water Resources, Yangling 712100, China

forces are revealed to be key factors that affect the stability of aggregates in an aqueous system (Li et al. 2013; Hu et al. 2015; Calero et al. 2017; Yu et al. 2017, 2020). Soil internal forces come from the interaction between charged soil particles and adjacent water molecules in solution, which can reach as high as 100–1000 atm, much higher than other forces, such as raindrop impact force (1–3 atm), slaking effect (< 1 atm), and osmotic stress (< 2.5 atm) (Nearing et al. 1987; Zaher et al. 2005; Hu et al. 2015). Soil internal forces include three forces, namely, electrostatic force, van der Waals force, and hydration force. Among these three forces, the electrostatic and hydration forces are repulsive, which mainly induce the breakdown of soil aggregates, while van der Waals force is attractive, which inhibits the dispersion of soil aggregates (Hu et al. 2015; Huang et al. 2016). Aggregate stability is dependent on the balance of electrostatic, hydration, and Van der Waals forces (Hu et al. 2015; Huang et al. 2016).

Under natural condition, soil aggregates are tightly bound together due to the strong van der Waals attractive force between soil particles in dry soils (Li et al. 2013). However, during rainfall or irrigation, soil solution is diluted; strong hydration repulsive force and electrostatic repulsive force build up rapidly among soil particles and break down soil aggregates. Previous studies showed that aggregate stability decreased with increasing electrostatic force and hydration force in simulated rainfall under laboratory conditions (Li et al. 2013, 2018). Hu et al. (2018a, b) quantitatively evaluated the contribution rates of soil internal forces on rainfall splash erosion and found that soil internal forces initiate soil aggregate breakdown and significantly affected splash erosion. Although it has demonstrated that soil internal forces have an important influence on the stability of aggregates, and the soil internal forces have been calculated quantitatively; the results are based on a simplified model soil system (specific cation-saturated aggregates), which can only represent part of the properties of natural soils. Therefore, it is time to study the influence of soil internal forces on the stability of aggregates in the natural soil systems.

Soils represent an extremely complex material with a large number of various anions and cations on their surface. In such circumstances, it remains challenging to quantitatively calculate the internal forces of natural soils. However, some studies employ ethanol to shield the soil internal forces with the aim to study the influence of external forces on some soil processes (Goebel et al. 2012; Hu et al. 2018b; Fu et al. 2019). For example, Hu et al. (2018b) utilized ethanol and electrolyte solutions with different concentrations as rainfall materials to quantitatively separate the effects of soil internal and raindrop impact forces (external) on splash erosion. Ethanol was used to represent the only effect of soil external forces on splash erosion. Meanwhile, an electrolyte solution was used to represent the integrated effects of soil internal and external forces on splash erosion. The obtained results showed that the contribution of soil internal forces to rainfall splash erosion is greater than that of raindrop impact force. Therefore, ethanol is proved to be a good choice to identify the soil internal forces and external forces. In addition, we know that when dry aggregates are fast wetted by deionized water, they will break down because of suffering strong repulsive soil internal forces. However, when dry aggregates are fast wetted by ethanol, the effect of soil internal forces on aggregates can be removed, and soil aggregate will maintain their original state. This phenomenon is due to the fact that ethanol can prevent slaking and swelling due to its weak polarizability and its relatively low surface tension (Concaret 1967; Le Bissonnais 1996). Besides, ethanol has a much smaller dielectric constant with respect to that of water (ethanol vs water 28.4 vs 78.4), which can compress the diffuse layer of particles (Lagaly and Ziesmer 2003) and lower the repulsive soil internal forces (Permien and Lagaly 1994). Therefore, the different properties between deionized water and ethanol can be used to evaluate the effect of soil internal forces on aggregate stability.

Soil internal forces are affected by the electrochemical properties of soil particles, such as soil cation exchange capacity (CEC) and specific surface area (SSA) (Li et al. 2013; Yu et al 2017). During vegetation restoration, the electrochemical properties of soil particles change with the change of soil basic properties, such as soil organic matter (SOM) content, pH, soil particle composition, and clay mineralogy (Hepper et al. 2006; Gruba and Mulder 2015; Liu et al. 2020). Hepper et al. (2006) reported that SSA was positively related with silt contents; organic matter losses due to excessive cultivation would decrease CEC. Liu et al. (2020) found that during the long-term natural grassland restoration, CEC and SSA increased with the increase of SOM and silt contents. Thus, in the process of vegetation restoration, soil internal forces, usually as high as 100–1000 atm, will change with the change of the electrochemical properties based on the classic double layer theory, which will further influence the stability of aggregates. However, the effect of soil internal forces on aggregate stability during vegetation restoration has not been reported, hindering our understanding of the formation and stabilization process of soil aggregates.

Therefore, in this study we investigated the stability of soil aggregates under different succession stages (farmland, grassland, shrubland, early forest, and climax forest) by dry sieving, and wet sieving with ethanol and deionized water prewetting. The purpose of dry sieving is to determine the size distribution and stability of dry aggregates and then compare them with the wet sieving. The wet sieving with ethanol and deionized water prewetting determines the size distribution and stability of wet aggregates in the presence or absence of soil internal forces. This work aims to evaluate

the effect of soil internal forces on the stability of natural soil aggregates during vegetation restoration.

2 Materials and methods

2.1 Study area

This study was conducted on the Lianjiabian Forest Farm, Heshui County, Gansu province, China (35°03′–36°37′N, 108°10′–109°18′E, 1211–1453 m a.s.l.). The location of the study area is present in the region of Ziwuling Forest in the hinterland of the Loess Plateau. The mean annual precipitation and temperature of the area were 587 mm and 7.4 °C, respectively, with a semi-arid monsoon climate. The main soil type is loessial soil (Calcaric Cambisols, WRB classification, 2014) (Jia et al. 2005). In this area, previous research revealed that the Ziwuling forest region is the sole intact natural secondary forest that remains on the Loess Plateau. A series of succession stages have been developed over the past 150 years with different restoration ages. The restoration successive series began from abandoned farmland and advanced as the order of grassland (*Bothriochloa ischaemum*, *Carex lanceolata*, *Glycyrrhiza*, and *Stipa bungeana*), shrubland (*Sophora davidii*, *Hippophae rhamnoides*, and *Spiraea pubescens*), early forest (*Populus davidiana* and *Betula platyphylla*), and climax forest (*Quercus liaotungensis*) stages (Deng et al. 2013).

2.2 Sampling and analysis

Field survey and sampling were conducted in mid-June 2018. Based on our previous investigation (Deng et al. 2013), a series of secondary vegetation succession was constructed by choosing five succession stages containing farmland, grassland, shrubland, early forest, and climax forest. Three sampling sites were selected as replicates for each vegetation community, and three plots (20 m × 20 m for forest community, 10 m × 10 m for shrubland community, and 1 m × 1 m for grassland community and farmland) were randomly established within each sampling site. In total, 45 samples (five succession stages × three sampling sites × three plots) were collected. Table 1 lists the basic information of these sites. After removing the surface leaf litter, soil samples were collected from the top layer of 0–20 cm in each plot. Meanwhile, the collection of undisturbed soil was made by cutting the ring (diameter and height of 5 cm each) to measure the bulk density (BD) of soil. After that, we air-dried the soil samples and removed the impurities such as roots and gravels in the soils. Then, we took a small part of soil samples, sieved through 2-mm and 0.25-mm screens, to determine the physicochemical properties of soil. Soil pH (solution/soil ratio: 5/1) was determined via pH meter (Leici, Shanghai, China), while detection of soil organic carbon (SOC) was conducted through the $K_2Cr_2O_7$ oxidation method (Kalembasa and Jenkinson 1973); CEC and SSA were studied with the combined method for surface property determination suggested by Li et al. (2011). Soil particle size distribution was determined using a Malvern Mastersizer 2000 laser diffraction equipment (Malvern Instruments Ltd, UK).

2.3 Experimental methods

Dry sieving was employed for the determination of the size distribution and stability of dry soil aggregates (Kemper and Rosenau 1986). The protocol involves even placing of air-dried samples (100 g) which have been sieved through a 5-mm sieve present on the top of a set of sieves with an opening of 2, 1, 0.5, 0.25, 0.15, and 0.053 mm from top to bottom, shaking by using a dry-sieving machine with a 75-stroke frequency for 5 min followed by the determination of the sample weight present on each sieve.

To determine the impact of soil internal forces on the aggregate stability, ethanol and deionized water were employed to fast wet the soil aggregates, and then the disintegrated aggregates were sieved in ethanol to obtain the

Table 1 Characteristics and location of the investigation sites (Ma et al. 2020)

Succession stages	Longitude	Latitude	Altitude (m)	Slope	Aspect	Coverage/canopy density (%)	Main plant species
Farmland	108°32′5.99″	36°4′36.20″	1021	0°	NE10°	—	—
Grassland	108°31′36.70″	36°5′3.13″	1345	13°	SE74°	95	*Bothriochloa ischaemum*, *Artemisia sacrorum*, *Stipabungeana*
Shrubland	108°31′36.02″	36°5′5.81″	1349	10°	NW30°	70	*Hippophae rhamnoides*, *Ostryopsis davidiana*, *Stipa bungeana bungeana*
Early forest	108°31′45.04″	36°2′54.57″	1449	12°	NW13°	68	*Populus davidiana*, *Betula platyphylla*, *Carex lanceolata*
Climax forest	108°32′32.37″	36°3′5.26″	1432	17°	NE51°	75	*Quercus liaotungensis*

size distribution and stability (Le Bissonnais 1996; Liu et al. 2014). The specific experimental steps are presented as follows: 50 g of mixed soil sample was matched according to the proportion of dry aggregate size, the soil sample gently immersed in ethanol or deionized water for 10 min, the excess ethanol or water piped out, and the remaining soil–water mixture transferred on topmost of a set of six sieves (2, 1, 0.5, 0.25, 0.15, and 0.053 mm) for the separation of aggregate fragments via the wet sieving method. To carry out the wet sieving, 99% ethanol was used to avoid the damage of the aggregate structure during the process of sieving and to inhibit the re-aggregation upon drying. The sieves were shaken in ethanol (amplitude 2 cm, moved up and down 10 times in 1 min) to obtain aggregate fractions of > 2, 2–1, 1–0.5, 0.5–0.15, 0.15–0.053, and < 0.053 mm. The aggregate stability obtained by wet sieving with deionized water prewetting was defined as the water stability of aggregates (Le Bissonnais 1996).

2.4 Index calculation

The mean weight diameter (MWD) and geometric mean diameter (GMD) are common indexes reflecting the soil aggregate stability. The larger the value, the stronger the stability of aggregates and the better agglomeration (Gardner 1956; Youker and McGuinness 1957). Those indices can be calculated according to formulas 1 and 2.

$$MWD = \sum_{i}^{n} x_i w_i / \sum_{i}^{n} w_i \tag{1}$$

$$GMD = exp\left(\sum_{i}^{n} w_i ln x_i / \sum_{i}^{n} w_i \right) \tag{2}$$

where w_i and x_i denote the proportion (%) and mean diameter (mm) of each aggregate size fraction, respectively.

The fractal dimension (D) is considered as a more credible and sensitive parameter. The more stable the soil granule structures, the smaller the fractal dimension (Tyler and Wheatcraft 1992). It can be calculated by Formulas 3 and 4.

$$W/W_T = \left(\bar{R}_i/R_{max}\right)^{3-D} \tag{3}$$

$$lgW/W_T = (3-D)lg\left(\bar{R}_i/R_{max}\right) \tag{4}$$

where $\bar{R}_i$ denotes the average diameter of each aggregate size class (mm), W is the weight of the aggregate < $\bar{R}_i$ (g), W_T is the total weight of the aggregates (g), and R_{max} represents the maximum diameter of the aggregates (mm).

The transfer matrix method is used to evaluate the preservation rate of individual aggregate size fractions (Shi 2006). The percentage of the aggregates that are placed in sieve i before wet-sieving constructs a matrix M_i, and the percentage of the aggregates that are placed in sieve i after wet-sieving constructs a matrix N_i. The probability of the original aggregates on each sieve preserved in the original sieve during sieving is X_1, X_2…, X_i and then $MX = N$. The sum of the preservation rate of each size is used as aggregate stability index (ASI). The ASI is an advanced tool used to analyze the soil aggregate stability. A larger ASI value represents higher aggregate stability (Niewczas and Witkowska-Walczak 2003).

The relative internal force index (RII) was adopted to estimate the impact of the soil internal forces on aggregate stability. The larger the RII, the greater the repulsive soil internal forces generated between soil particles and the greater the degree of disintegration of aggregates. The RII was calculated by following Formula 5.

$$RII = \frac{MWDe - MWDw}{MWDe} \times 100\% \tag{5}$$

where MWDe is mean weight diameter determined via wet sieving with ethanol prewetting and MWDw is mean weight diameter determined via wet sieving with deionized water prewetting.

2.5 Statistical analysis

In this study, all the statistical analyses were carried out with SPSS statistical software version 19.0. Treatment differences were determined by two-way analysis of variance (ANOVA) in combination with the LSD test. The significance level of the data was set to 0.05. Origin 9.0 was employed to visualize the data.

3 Results

3.1 Basic soil properties under different succession stages

Table 2 shows the basic soil physicochemical properties. The soils in different succession stages were alkaline with pH values ranging from 8.34 to 8.49. Soil BD decreased gradually from 1.27 to 1.04 g cm^{-3}, decreasing by 18.1%, with vegetation succession. The SOC content increased from 7.20 to 16.93 g kg^{-1}, increasing by 135.1%, with vegetation succession. The CEC and SSA increased from 10.90 to 19.52 cmol kg^{-1} and from 43.92 to 61.39 m^2 g^{-1}, respectively. Soil particle composition changed slightly along with the restoration stages, i.e., sand content decreases and silt and clay content increases.

Table 2 Basic properties of testing soil (Ma et al. 2020)

Succession stages	pH	BD (g cm^{-3})	SOC (g kg^{-1})	CEC (cmol kg^{-1})	SSA (m^2 g^{-1})	Soil particle composition (%)		
						Sand 2–0.02 mm	Silt 0.02–0.002 mm	Clay < 0.002 mm
Farmland	8.34	1.27	7.20	10.90	43.92	53.20	28.43	18.37
Grassland	8.46	1.26	9.14	15.54	53.01	51.43	28.51	20.06
Shrubland	8.38	1.17	12.73	16.60	55.30	50.46	29.03	20.51
Early forest	8.49	1.11	14.18	17.87	59.17	48.87	29.94	21.19
Climax forest	8.39	1.04	16.93	19.52	61.39	47.69	30.33	21.98

BD bulk density, *SOC* soil organic carbon, *CEC* cation exchange capacity, *SSA* specific surface area

3.2 Size distribution and stability of soil aggregates under different succession stages

3.2.1 Size distribution and stability of soil aggregates determined by dry sieving

Figure 1 shows the size distribution of dry aggregates. As shown in Fig. 1, the percentage of different particle sizes aggregates in different succession stages was higher in the 5–2-, 2–1-, 0.15–0.053-, and < 0.053-mm fraction, followed by 1–0.5-mm and 0.5–0.25-mm fraction, the 0.25–0.15-mm fraction being the lowest. Decreasing particle size represented that the percentage of different particle sizes aggregates presents a "V"-type change trend that decreases first and then increases. Besides, with vegetation restoration, the percentage of 5–2-mm aggregates was significantly increased, while the percentage of 0.15–0.053-mm and < 0.053-mm aggregates was significantly decreased, and no significant change was observed for the percentage of 0.25–0.15-mm aggregates.

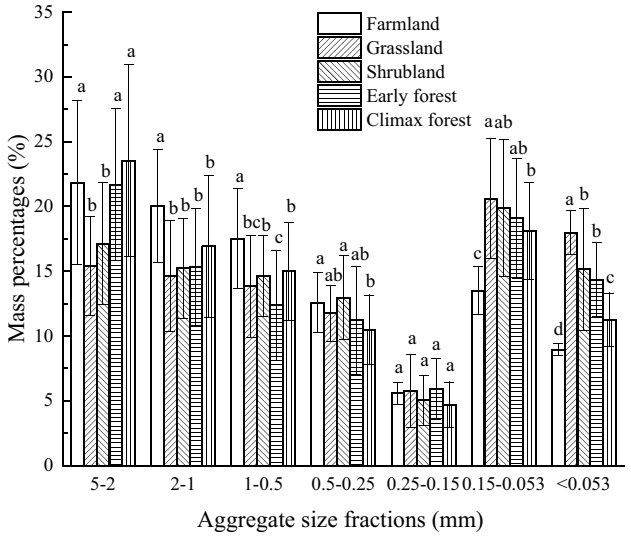

Fig. 1 Soil aggregate size distribution under different succession stages determined by dry sieving. The error bars represent the standard deviations of the means ($n = 3$). The different lowercase letters indicate significant differences between different succession stages at $P < 0.05$

Table 3 shows the variation of the dry aggregate stability under different succession stages. In Table 3, the highest MWD values were observed in farmland and climax forest followed by early forest. The lowest values were found in shrubland and grassland. The highest values of GMD were observed in farmland followed by climax forest, and the lowest values occurred in grassland. D showed the reverse order of MWD and GMD values, and decreased in the following order: grassland > shrubland > early forest > climax forest > farmland.

3.2.2 Size distribution and stability of soil aggregates determined by wet sieving with ethanol prewetting

Figure 2 shows the soil aggregate size distribution measured by wet sieving with ethanol prewetting. As shown in Fig. 2, the percentage of different particle size aggregates in different succession stages was higher in the < 0.053-, 0.15–0.053-, and 5–2-mm fraction, followed by the 2–1-, 1–0.5-, and 0.5–0.25-mm fraction, while it was the lowest in the 0.25–0.15-mm fraction. With decreasing particle size, the percentage of different particle sizes aggregates

Table 3 The stability of dry aggregates under different succession stages determined by dry sieving

Succession stages	MWD (mm)	GMD (mm)	D
Farmland	1.27 ± 0.33a	0.58 ± 0.12a	2.47 ± 0.10d
Grassland	0.94 ± 0.26c	0.33 ± 0.08e	2.64 ± 0.15a
Shrubland	1.02 ± 0.19bc	0.38 ± 0.06d	2.60 ± 0.11b
Early forest	1.10 ± 0.22b	0.42 ± 0.10c	2.59 ± 0.10b
Climax forest	1.26 ± 0.28a	0.51 ± 0.08b	2.53 ± 0.08c

Means ± standard deviations ($n = 3$). The different lowercase letters indicate significant differences between different succession stages at $P < 0.05$

MWD mean weight diameter, *GMD* geometric mean diameter, *D* fractal dimension

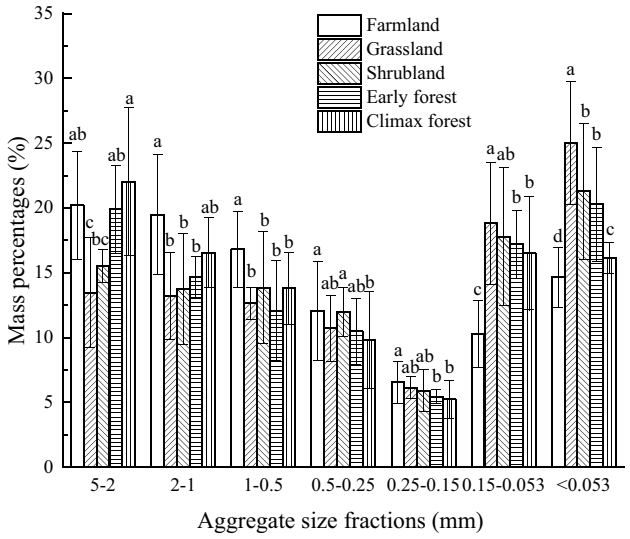

Fig. 2 Soil aggregate size distribution under different succession stages determined by wet sieving with ethanol prewetting. The error bars represent the standard deviations of the means ($n=3$). The different lowercase letters indicate significant differences between different succession stages at $P<0.05$

presents a "V"-type change trend that decreases first and then increases. Besides, with vegetation restoration, the percentage of 5–2-mm aggregates was significantly enhanced, and the percentage of 0.25–0.15-, 0.15–0.053-, and < 0.053-mm aggregates was significantly decreased.

Table 4 shows the variation of soil aggregate stability under different succession stages determined by the wet sieving with ethanol prewetting. In Table 4, the highest values of MWDe occurred in farmland and climax forest followed by early forest. The lowest values were found in shrubland and grassland. The highest values of GMD appeared in farmland and climax forest followed by early forest and shrubland, and the lowest values occurred in grassland. D showed the reverse order of MWDe and GMD values, and decreased

Table 4 Soil aggregate stability under different succession stages determined by wet sieving with ethanol prewetting

Succession stages	MWDe (mm)	GMD (mm)	D
Farmland	1.20 ± 0.24a	0.49 ± 0.17a	2.54 ± 0.07c
Grassland	0.84 ± 0.18c	0.26 ± 0.06c	2.70 ± 0.11a
Shrubland	0.93 ± 0.15bc	0.31 ± 0.11bc	2.66 ± 0.09ab
Early forest	1.08 ± 0.19ab	0.35 ± 0.08b	2.64 ± 0.10ab
Climax forest	1.19 ± 0.21a	0.43 ± 0.15a	2.59 ± 0.05bc

Means ± standard deviations ($n=3$). The different lowercase letters indicate significant differences between different succession stages at $P<0.05$

MWDe mean weight diameter determined by wet sieving with ethanol prewetting, *GMD* geometric mean diameter, *D* fractal dimension

in the following order: grassland > shrubland > early forest > climax forest > farmland.

3.2.3 Size distribution and stability of soil aggregates determined by wet sieving with deionized water prewetting

Figure 3 shows the soil aggregate size distribution measured by wet sieving with deionized water prewetting. As shown in Fig. 3, the percentage of different particle size water-stable aggregates under different succession stages was higher in the < 0.15-mm fraction, followed by 5–0.25-mm fraction, while lowest in the 0.25–0.15-mm fraction. Compared to size distribution investigated by the ethanol prewetting, the process of fast wetting in deionized water increased the percentage of < 0.25-mm aggregates, and decreased the percentage of > 0.25-mm aggregates. Also, vegetation restoration significantly increased the percentage of 5–2- and 2–1-mm aggregates, and decreased the percentage of 0.15–0.053- and < 0.053-mm aggregates.

Table 5 shows the variation of water stability of soil aggregates during vegetation restoration. In Table 5, the MWDw and GMD values showed the same varying tendencies, all of which were increased with vegetation restoration. The highest values of MWDw and GMD were observed in climax forest, followed by early forest, shrubland, and grassland. The lowest values appeared in farmland. However, the D displayed the opposite trend of MWDw and GMD, which was decreased with vegetation restoration.

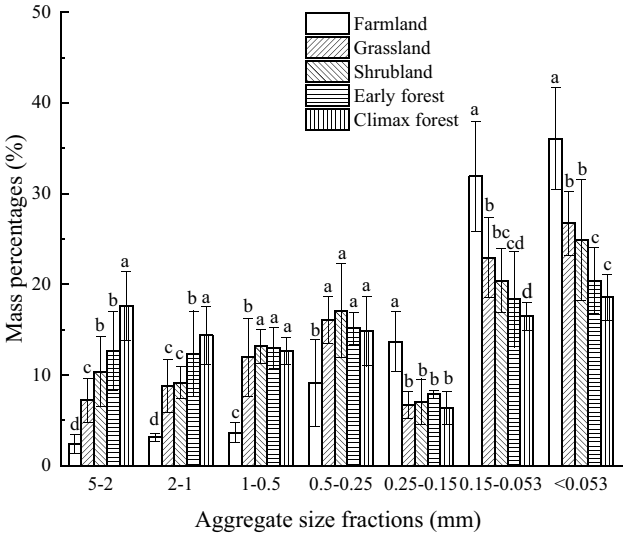

Fig. 3 Soil aggregate size distribution under different succession stages determined by wet sieving with deionized water prewetting. The error bars represent the standard deviations of the means ($n=3$). The different lowercase letters indicate significant differences between different succession stages at $P<0.05$

Table 5 Soil aggregate water stability under different succession stages determined by wet sieving with deionized water prewetting

Succession stages	MWDw (mm)	GMD (mm)	D
Farmland	0.26 ± 0.04d	0.10 ± 0.02d	2.84 ± 0.05a
Grassland	0.58 ± 0.07c	0.19 ± 0.04c	2.74 ± 0.07b
Shrubland	0.71 ± 0.13bc	0.22 ± 0.08bc	2.70 ± 0.07bc
Early forest	0.82 ± 0.16b	0.28 ± 0.10ab	2.66 ± 0.08 cd
Climax forest	1.02 ± 0.17a	0.35 ± 0.11a	2.62 ± 0.03d

Means ± standard deviations ($n = 3$). The different lowercase letters indicate significant differences between different succession stages at $P < 0.05$

MWDw mean weight diameter determined by wet sieving with deionized water prewetting, *GMD* geometric mean diameter, *D* fractal dimension

3.3 Preservation rate of soil aggregates and ASI under different succession stages

As shown in Table 6, the higher preservation rate of individual aggregate size fractions was observed in 0.5–0.25-, 0.25–0.15-, and 0.15–0.053-mm aggregates and the lower preservation rate was found in 5–2-, 2–1-, and 1–0.5-mm aggregates, suggesting that soil internal forces exert less effect on the particle size 0.5–0.053-mm fractions, which mainly break down the particle size > 0.5-mm fraction. The preservation rate in each fraction and ASI was increased with the process of vegetation restoration. The ASI values of grassland, shrubland, early forest, and climax forest were 1.93, 2.22, 2.45, and 2.48 times of that of farmland, respectively.

3.4 Effect of soil internal forces on the stability of soil aggregates during vegetation restoration

The RII was adopted to estimate the effect of soil internal forces on aggregate stability. As shown in Fig. 4, the RII was decreased with vegetation restoration, and the RII of grassland, shrubland, early forest, and climax forest decreased by 47%, 54%, 55%, and 64% compared with that of farmland, respectively. The results indicated that vegetation restoration process decreased the degree of disintegration of the aggregates caused by soil internal forces.

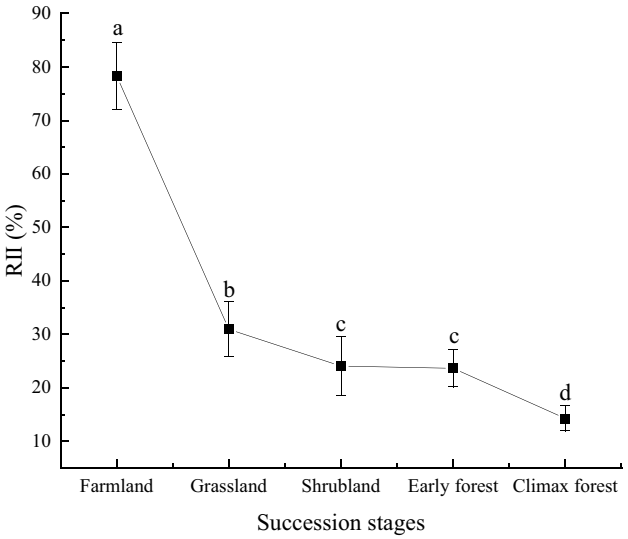

Fig. 4 Relative internal forces index (RII) under different succession stages. The error bars represent the standard deviations of the means ($n = 3$). The different lowercase letters indicate significant differences between different succession stages at $P < 0.05$

4 Discussion

Vegetation restoration can significantly improve soil physicochemical properties (Li and Shao 2006; Lenka et al. 2012; Deng et al. 2013; Bienes et al. 2016). In this study, the SOC content increased and soil BD decreased with vegetation restoration, which were consistent with the findings reported previously (Burri et al. 2009; Dou et al. 2020). Vegetation restoration increases the amount of vegetation biomass, and large quantities of leaf litter and plant residues are associated with the enhancement of soil fertility, the

Table 6 Preservation rate and of soil aggregates and ASI

Succession stages	Preservation rate of individual aggregate size fractions							ASI
	5–2 (mm)	2–1 (mm)	1–0.5 (mm)	0.5–0.25 (mm)	0.25–0.15 (mm)	0.15–0.053 (mm)	< 0.053 (mm)	
Farmland	0.12	0.08	0.07	0.15	0.24	0.60	1.00	2.27
Grassland	0.54	0.45	0.51	0.73	0.55	0.95	1.00	4.73
Shrubland	0.67	0.49	0.56	0.77	0.63	0.93	1.00	5.05
Early forest	0.68	0.63	0.64	0.79	0.87	0.96	1.00	5.57
Climax forest	0.75	0.67	0.61	0.83	0.80	0.97	1.00	5.63

The preservation rate is obtained through constructing two matrices between the results of ethanol treatment and deionized water treatment

ASI aggregate stability index

development of physical characteristics, and the improvement of the soil structure (Li and Shao 2006). Besides, the surface charge properties of soil particles, such as CEC and SSA, increased during vegetation restoration, which was in agreement with the conclusion of Liu et al. (2020). Changes in surface charge properties of soil particles may be associated with the increase of organic matter content during vegetation restoration. SOM is a kind of colloidal particles, which has a lot of surface charges (300–600 cmol kg^{-1}) and a high specific surface area (500–800 m^2 g^{-1}) (Leinweber et al. 1993; Pennell et al. 1995). SOM transferred into the soil can bind to the mineral particle surface through chemical bonding and form organo-mineral complexes. The interaction between SOM and clay minerals can greatly alter soil particle surface charge properties (Thompson et al. 1989; Oorts et al. 2003).

The results of dry sieving revealed that revegetation favored the macroaggregate (1–5 mm) formation and promoted the stability of the dry aggregates. This was consistent with the findings obtained by Tang et al. (2016) and Mahesh et al. (2017) who suggested that vegetation restoration promoted the accumulation of aggregates with small particle sizes into large sizes due to the increase of SOM content. The stability of dry aggregates was higher in farmland, which was due to the fact that long-term application of inorganic fertilizer and continuous tillage caused the soil structure to be destroyed and compacted (Haynes and Naidu 1998; Wang et al. 2015). In addition, the results of the aggregate size distribution and stability determined by dry sieving were similar as those determined by wet sieving with ethanol prewetting, both showing that with the decrease of particle size, the percentage of different particle size aggregates decreased first and then increased, and the indexes of aggregate stability, including MWD, GMD, and D, also showed the same change rule with vegetation restoration. These results indicated that ethanol could shield soil internal forces and remove the influence of soil internal forces on soil aggregates, consequently maintaining soil aggregates in their original state (Le Bissonnais 1996; Lagaly and Ziesmer 2003). Besides, the MWD and GMD measured by wet sieving in ethanol treatment were slightly smaller than by dry sieving and the D measured by wet sieving in ethanol treatment was slightly larger than that by dry sieving. This is due to the smaller agitating force used in the process of wet sieving that exerts an effect on aggregate stability.

The results of wet sieving in deionized water prewetting demonstrated that vegetation restoration increased the content of water-stable macroaggregate (1–5 mm) and decreased the content of water-stable microaggregate (< 0.15 mm), and increased the water stability of soil aggregates. These results were consistent with previous researches (Lenka et al. 2012; Liu et al. 2014). These results are commonly attributed to the increase of organic matter content, since SOM performs the function of binding agent, contributing to aggregate stabilization and formation through binding soil mineral particles (Chaplot and Cooper 2015). Besides, plant roots are also involved in the formation and stabilization of soil aggregates. Fine roots interact with external hyphae and generate exudates and temporary binding agents, promoting the soil aggregate formation (Six et al. 2004; Eisenhauer et al. 2011). Additionally, certain studies authenticated that afforestation could stimulate the activity and growth of microorganisms and yield transient binding agents required for the agglomeration, which could thus affect soil aggregate stability (Six et al. 2000; Zhu et al. 2017).

In addition to the above factors, soil internal forces also exert an important impact on the stability of aggregates. Our results showed that the fast wetting process in deionized water increased the percentage of < 0.25-mm aggregates, and decreased the percentage of > 0.25-mm aggregates, and the aggregate stability in ethanol treatment was higher than that in deionized water treatment. For instance, the MWDe values of farmland, grassland, shrubland, early forest, and climax forest soils were 4.62, 1.45, 1.31, 1.32, and 1.17 times of their MWDw values. The higher aggregate stability in ethanol treatment than that in deionized water treatment was due to the fact that ethanol can reduce the influence of soil internal forces on soil aggregates and maintain soil aggregates in their original state (Le Bissonnais 1996; Lagaly and Ziesmer 2003). By contrast, soil aggregates in deionized water treatment suffered strong repulsive soil internal forces and disintegrated severely (Li et al. 2013; Hu et al. 2015). Therefore, the MWDw values were significantly lower than MWDe values. These results indicated that the repulsive soil internal forces significantly broke down the aggregates. Many studies have investigated the effect of soil internal forces on soil aggregate stability. They used model soil systems demonstrated that soil internal forces could produce interparticle forces as high as 100–1000 atm, and significantly affect aggregate stability (Li et al. 2013; Hu et al. 2015; Gong et al. 2018). In the current work, we also prove that soil internal forces have an important influence on the stability of aggregates in natural soil systems. Unfortunately, due to the complexity of soil systems, we can only qualitatively evaluate the effect of soil internal forces on aggregate stability. In addition, our results also showed that soil internal forces mainly broke down the particle size > 0.5-mm fraction. This result was similar to the outcomes of Niewczas and Witkowska-Walczak (2003). The reason is that the > 0.5-mm aggregates are more prone to degradation by water erosion, since the erosion can physically disrupt the formation of water-stable aggregates with larger sizes (Ayoubi et al. 2012).

During the process of vegetation restoration, soil internal forces will change with the change of soil properties. Our results showed that RII decreased with vegetation

restoration, indicating that the vegetation restoration process decreased the repulsive soil internal forces, thereby decreasing the degree of disintegration of aggregates. The reason for the decrease of soil internal forces may be associated with SOM accumulation during the process of vegetation recovering. SOM accumulation can increase soil CEC and SSA (Table 2), which in turn can increase electrostatic repulsive force and more importantly increase the van der Waals attractive force between soil particles, finally decreasing the net repulsive force of soil internal forces and increasing aggregate stability (Thompson et al. 1989; Oorts et al. 2003; Huang 2004; Hu et al. 2015; Liu et al. 2020). A similar result was also reported by Yu et al. (2017), who found that the increase of soil organic matter content through straw incubation would greatly increase the interparticle attractive forces, resulting in the decrease of the repulsive soil internal forces and ultimately improve soil aggregate stability. Therefore, it may be that the increase of organic matter content in the process of vegetation restoration reduces the repulsive soil internal forces and thus the aggregate stability is improved.

5 Conclusions

In this study, we qualitatively evaluated the effect of soil internal forces on the stability of natural soil aggregates during vegetation restoration with ethanol and deionized water. The results showed that soil aggregates would not break down as they were fast wetted in ethanol because of removal of the effect of soil internal forces, while soil aggregates would severely break down as they were fast wetted in deionized water due to suffering strong repulsive soil internal forces, and the soil internal forces mainly broke down > 0.5-mm aggregates during fast wetting. Moreover, it could also be found that with the vegetation restoration, the degree of disintegration of aggregates caused by soil internal forces decreased; thus, the water stability of aggregates increased. The obtained findings reveal the reasons for the improvement of water stability of aggregates in the process of vegetation restoration from the perspective of soil internal forces, and provide theoretical references for further study of the formation and stability of good soil structure.

Funding This work was supported by the National Natural Science Foundation of China (41977024, 41601236) and the Fundamental Research Funds for the Central Universities (2452019078).

References

Ayoubi S, Karchegani PM, Mosaddeghi MR, Honarjoo N (2012) Soil aggregation and organic carbon as affected by topography and land use change in western iran. Soil Tillage Res 121:18–26

Bienes R, Marques MJ, Sastre B, García-Díaz A, Ruiz-Colmenero M (2016) Eleven years after shrub revegetation in semiarid eroded soils Influence in soil properties. Geoderma 273:106–114

Burri K, Graf F, Albert B (2009) Revegetation measures improve soil aggregate stability: a case study of a landslide area in Central Switzerland. For Snow Landscape Res 82:45–60

Calero J, Ontiveros-Ortega A, Aranda V, Plaza I (2017) Humic acid adsorption and its role in colloidal-scale aggregation determined with the zeta potential, surface free energy and the extended-DLVO theory. Eur J Soil Sci 68:491–503

Chaplot V, Cooper M (2015) Soil aggregate stability to predict organic carbon outputs from soils. Geoderma 243:205–213

Concaret J (1967) Etude des mécanismes de destruction des agrégats de terre au contact de solutions aqueuses. Ann Agronom 18:99–144

Deng L, Wang KB, Chen ML, Shangguan ZP, Sweeney S (2013) Soil organic carbon storage capacity positively related to forest succession on the Loess Plateau, China. Catena 110:1–7

Dou YX, Yang Y, An SS, Zhu ZL (2020) Effects of different vegetation restoration measures on soil aggregate stability and erodibility on the Loess Plateau, China. Catena 185

Eisenhauer N, Milcu A, Sabais ACW, Bessler H, Brenner J, Engels C, Klarner B, Maraun M, Partsch S, Roscher C (2011) Plant diversity surpasses plant functional groups and plant productivity as driver of soil biota in the long term. PLos One 6: e16055

El Kateb H, Zhang H, Zhang P, Mosandl R (2013) Soil erosion and surface runoff on different vegetation covers and slope gradients: a field experiment in Southern Shaanxi Province. Catena 105:1–10

Fu Y, Li GL, Zheng TH, Zhao YS, Yang MY (2019) Fragmentation of soil aggregates induced by secondary raindrop splash erosion. Catena 185:104342

Gardner WR (1956) Representation of soil aggregate-size distribution by a logarithmic-normal distribution. Soil Sci Soc Am Proc 20:151–153

Goebel MO, Woche SK, Bachmann J (2012) Quantitative analysis of liquid penetration kinetics and slaking of aggregates as related to solid–liquid interfacial properties. J Hydrol 442–443:63–74

Gong Y, Tian R, Li H (2018) Coupling effects of surface charges, adsorbed counterions and particle-size distribution on soil water infiltration and transport. Eur J Soil Sci 69:1008–1017

Gruba P, Mulder J (2015) Tree species affect cation exchange capacity (CEC) and cation binding properties of organic matter in acid forest soils. Sci Total Environ 511:655–662

Haynes RJ, Naidu R (1998) Influence of lime, fertilizer and manure applications on soil organic matter content and soil physical conditions: a review. Nutr Cycl Agroecosyst 51:123–137

Hepper EN, Buschiazzo DE, Hevia GG, Urioste A, Antón L (2006) Clay mineralogy, cation exchange capacity and specific surface area of loess soils with different volcanic ash contents. Geoderma 135:216–223

Hu FN, Xu CY, Li H, Li S, Yu ZH, Li Y, He XH (2015) Particles interaction forces and their effects on soil aggregates breakdown. Soil Tillage Res 147:1–9

Hu FN, Liu JF, Xu CY, Du W, Yang ZH, Liu XM, Liu G, Zhao SW (2018a) Soil internal forces contribute more than raindrop impact force to rainfall splash erosion. Geoderma 330:91–98

Hu FN, Liu JF, Xu CY, Wang ZL, Liu G, Li H, Zhao SW (2018b) Soil internal forces initiate aggregate breakdown and splash erosion. Geoderma 320:43–51

Huang PM (2004) Soil mineral-organic matter-microorganism interactions: fundamentals and impacts. Adv Agron 82:391–472

Huang XR, Li H, Li S, Xiong HL, Jiang XH (2016) Role of cationic polarization in humus-increased soil aggregate stability. Eur J Soil Sci 67:341–350

IUSS Working Group WRB (2014) World reference base for soil resources 2014. International Soil Classification System for

Naming Soils and Creating Legends for Soil Maps. World Soil Resources Reports No. 106. FAO, Rome.
Jia GM, Cao J, Wang CY, Wang G (2005) Microbial biomass and nutrients in soil at the different stages of secondary forest succession in Ziwuling, northwest China. For Ecol Manag 217:117–125
Kalembasa SJ, Jenkinson DS (1973) A comparative study of titrimetric and gravimetric methods for the determination of organic carbon in soil. J Sci Food Agric 24:1085–1090
Kemper DW, Rosenau RC (1986) Aggregate stability and size distribution A. Klute (Ed.), Methods of soil analysis, part 1, American Society of Agronomy, Madison (WI) 425–442
Kinnell PIA (2005) Raindrop-impact-induced erosion processes and prediction: a review. Hydrol Process 19:2815–2844
Lagaly G, Ziesmer S (2003) Colloid chemistry of clay minerals: the coagulation of montmorillonite dispersions. Adv Colloid Interf Sci 100:105–128
Le Bissonnais Y (1996) Aggregate stability and assessment of soil crustability and erodibility: I. Theory and methodology. Eur J Soil Sci 4:425–437
Leinweber P, Reuter G, Brozio K (1993) Cation exchange capacities of organo-mineral particle-size fractions in soils from long- term experiments. J Soil Sci 44:111–119
Lenka NK, Choudhury PR, Sudhishri S, Dass A, Patnaik US (2012) Soil aggregation, carbon build up and root zone soil moisture in degraded sloping lands under selected agroforestry based rehabilitation systems in eastern India. Agric Ecosyst Environ 150:54–62
Li H, Hou J, Liu XM, Li R, Zhu HL, Wu LS (2011) Combined determination of specific surface area and surface charge properties of charged particles from a single experiment. Soil Sci Soc Am J 75:2128–2135
Li S, Li H, Xu CY, Huang XR, Xie DT, Ni JP (2013) Particle interaction forces induce soil particle transport during rainfall. Soil Sci Soc Am J 77:1563–1571
Li S, Li Y, Huang XR, Hu FN, Liu XM, Li H (2018) Phosphate fertilizer enhancing soil erosion: effects and mechanisms in a variably charged soil. J Soil Sediments 18:863–873
Li YY, Shao MA (2006) Change of soil physical properties under long-term natural vegetation restoration in the Loess Plateau of China. J Arid Environ 64:77–96
Liu JF, Wang ZL, Hu FN, Xu C, Ma RT, Zhao SW (2020) Soil organic matter and silt contents determine soil particle surface electrochemical properties across a long-term natural restoration grassland. Catena 190:104526
Liu MY, Chang QR, Qi YB, Liu J, Chen T (2014) Aggregation and soil organic carbon fractions under different land uses on the tableland of the Loess Plateau of China. Catena 115:19–28
Ma RT, Hu FN, Liu JF, Xu CY, Yang ZH, Wang ZL, Zhao SW (2020) Evolution of soil surface electrochemical characteristics with vegetation restoration on Loess Plateau in Ziwuling area. Acta Pedologica Sinica 57:392–402 (in Chinese with English abstract)
Mahesh KS, Sunil S, Ghosha N (2017) Impact of land use change on soil aggregate dynamics in the dry tropics. Restor Ecol 25:962–971
Nearing MA, Bradford JM, Holtz RD (1987) Measurement of waterdrop impact pressures on soil surfaces. Soil Sci Soc Am J 51:1302–1306
Niewczas J, Witkowska-Walczak B (2003) Index of soil aggregates stability as linear function value of transition matrix elements. Soil Tillage Res 70:121–130
Oorts K, Vanlauwe B, Merckx R (2003) Cation exchange capacities of soil organic matter fractions in a Ferric Lixisol with different organic matter inputs. Agric Ecosyst Environ 100:161–171
Pennell KD, Abriola LM, Boyd SA (1995) Surface area of soil organic matter reexamined. Soil Sci Soc Am J 59:1012–1018
Permien T, Lagaly G (1994) The rheological and colloidal properties of bentonite dispersions in the presence of organic compounds III. The effect of alcohols on the coagulation of sodium montmorillonite. Colloid Polym Sci 272:1306–1312
Shi H (2006) Using transition matrix to evaluate stability of soil aggregates. Bull Soil Water Conserv 3:91–95
Six J, Bossuyt H, Degryze S, Denef K (2004) A history of research on the link between (micro) aggregates, soil biota, and soil organic matter dynamics. Soil Tillage Res 79:7–31
Six J, Paustian K, Elliott E, Combrink C (2000) Soil structure and organic matter I. Distribution of aggregate-size classes and aggregate-associated carbon. Soil Sci Soc Am J 64:681–689
Tang FK, Cui M, Lu Q, Liu YG, Guo HY, Zhou JX (2016) Effects of vegetation restoration on the aggregate stability and distribution of aggregate-associated organic carbon in a typical karst gorge region. Solid Earth 7:2213–2242
Thompson ML, Zhang H, Kazemi M, Sandor JA (1989) Contribution of organic matter to cation exchange capacity and specific surface area of fractionated soil material. Soil Sci 148:250–257
Tisdall JM, Oades JM (1982) Organic matter and water-stable aggregates in soil. J Soil Sci 33:141–163
Tyler SW, Wheatcraft SW (1992) Fractal scaling of soil-particle size distributions: analysis and limitations. Soil Sci Soc Am J 56:362–369
Wang XJ, Jia ZK, Liang LY, Yang BP, Ding RX, Nie JF, Wang JP (2015) Maize straw effects on soil aggregation and other properties in arid land. Soil Tillage Res 153:131–136
Youker RE, McGuinness JL (1957) A short method of obtaining mean weight diameter values of aggregate analyses of soils. Soil Sci 83:291–294
Yu ZH, Zhang JB, Zhang CZ, Xin XL, Li H (2017) The coupling effects of soil organic matter and particle interaction forces on soil aggregate stability. Soil Tillage Res 174:251–260
Yu ZH, Zheng YY, Zhang JB, Zhang CZ, Ma DH, Chen L, Cai TY (2020) Importance of soil interparticle forces and organic matter for aggregate stability in a temperate soil and a subtropical soil. Geoderma 362:114088
Zaher H, Caron J, Ouaki B (2005) Modeling aggregate internal pressure evolution following immersion to quantify mechanisms of structural stability. Soil Sci Soc Am J 69:1–12
Zhu GY, Shangguan ZP, Deng L (2017) Soil aggregate stability and aggregate-associated carbon and nitrogen in natural restoration grassland and Chinese red pine plantation on the Loess Plateau. Catena 149:253–260